ANNALS OF THE UNIVERSITY OF CRAIOVA

Series: ✓*Biology*
✓*Horticulture*
✓*Food products processing technology*
✓*Environmental engineering*

Vol. XXXI (LXVII) - 2026

THE HOLBINA-RAZIM SYSTEM, A TESTBED FOR SENTINEL-3 SATELLITE CALIBRATION FOR DELTAIC PHYCOCYANIN-DOMINATED SEVERE ALGAL BLOOMS

Gherman Vasile Daniel[1], Cimpoiasu Vily Marius[2], Ungureanu Laurenția[3], Zubcov Elena[3], Lebedenco Liubovi[3], Tumanova Daria[3], Bagrin Nina[3], Popa Radu[4]*

[1] University Politehnica of Timișoara, Faculty of Civil Engineering, Department of Hydrotechnics, Spiru Haret Street, no. 1A, Timișoara, Romania.

[2] University of Craiova, Faculty of Horticulture, Biology and Environmental Engineering Department, A.I. Cuza Street, no 13, Craiova, Romania.

[3] State University of Moldova. 60, Alexei Mateevici St., Republic of Moldova.

[4] National University, 9388 Lightwave Ave, San Diego, CA 92123, USA.

** Corresponding author. E-mail*: radu.o.popa@gmail.com.

Keywords*: Algal pigments, Chlorophyll, Phycocyanin, Remote sensing validation, Holbina-Razim, Surface algal bloom.*

ABSTRACT

The Holbina–Razim lake system serves as a calibration testbed for satellite-based algal pigment analysis during severe algal blooms (SABs) in deltaic environments. We demonstrate the reliability of this environment for field-to-satellite comparisons by integrating an 8-year historical dataset with in-situ measurements from a 2026 cyanobacterial SAB. Spatial gradients of chlorophyll-a and phycocyanin were validated against Sentinel-3 Normalized Difference Chlorophyll Index (NDCI) and Phycocyanin Index (PCI) parameters. Our findings confirm that the Holbina–Razim system provides a robust, scalable framework to benchmark remote sensing algorithms for phycocyanin in highly eutrophic, deltaic waters globally.

INTRODUCTION

Eutrophic pollution and climate warming lead to frequent, severe algal blooms (SABs) in aquatic ecosystems globally (Sinha et al. 2017). In freshwater lakes, SABs serve as rapid indicators of trophic degradation. Understanding how ecosystems respond to and recover from these events is a primary focus of anthropogenic ecology (Hu et al. 2024). However, monitoring these blooms in near-real time across vast spatial scales remains a major challenge. Algal blooms cover large surface areas, vary widely in intensity and taxonomic composition, and can shift within days—demanding frequent, precise, and multi-parameter ecological assessments.

Spaceborne remote sensing offers a powerful solution to these monitoring constraints. Yet, bridging the gap between satellite observations and in-situ reality requires rigorous validation in dedicated testbed environments. We propose the ~100 km² Holbina–Razim aquatic system in Romania as a model environment representing shallow, deltaic, freshwater temperate lakes. Although functioning as a continuous hydrographic unit, this system has maintained a distinct, steady spatial gradient in SAB distribution for at least eight years (Fig. 1). This environmental consistency makes the Holbina–Razim system an excellent natural laboratory to validate satellite-derived observations against direct field measurements of chlorophyll-a (Chl-a) and phycocyanin (Phy). We compared in-situ Chl-a and Phy concentrations, measured via in-vivo fluorescence within the 0.4–0.5 m epilimnion, with remote sensing surface reflectance data acquired at daily intervals by the Sentinel-3 satellite constellation and converted into two spectral pigment parameters: the Normalized Difference Chlorophyll Index (NDCI) and the Phycocyanin Index (PCI).

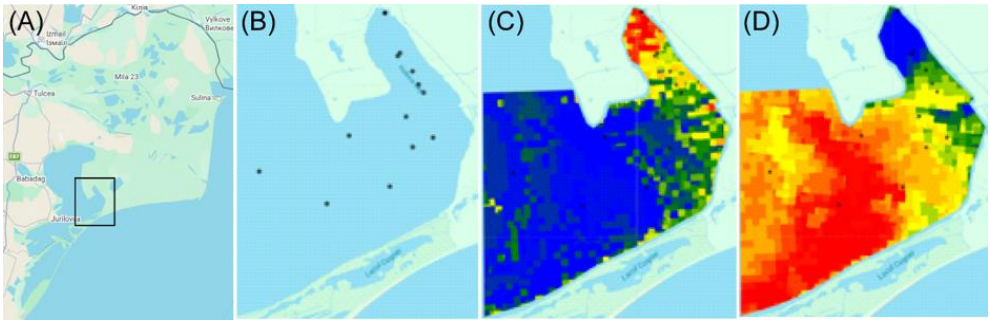


Figure 1. (A) Location of the Holbina–SE_Razim study area within the Danube Delta (indicated by the black rectangle). (B) Spatial distribution of the 14 field sampling stations investigated for chlorophyll-a (Chl-a) and phycocyanin (Phy). (C) Multi-temporal average distribution of Sentinel-3 NDCI values used as a Chl-a proxy. (D) Multi-temporal average distribution of Sentinel-3 PCI values used as a Phy proxy. The maps in (C) and (D) illustrate pixel-based averages generated in Google Earth Engine (GEE) using the Sentinel-3 library for the period 11 August 2018 to 13 August 2026. In panel (C), blue pixels denote high NDCI values (indicative of high [Chl-a]) and red pixels denote low NDCI values (indicative of low [Chl-a]), spanning a color palette range between -0.08 and -0.04. In panel (D), blue pixels correspond to low PCI values (low [Phy]) and red pixels signify high PCI values (high [Phy]), mapped across a palette range of 0.7–0.8.

MATERIALS AND METHODS

A large-scale severe algal bloom (SAB), covering an area exceeding 200 km², occurred within the Razim Lake system (Romania) during early to mid-August 2026. This bloom was investigated in the southeastern portion of Razim Lake and within Holbina Bay, which forms an interconnected part of the broader lake system (Fig. 1). Field sampling was conducted over two days (11 and 13 August 2026) during the peak phase of the bloom. Sampling dates were selected based on clear, sunny conditions with minimal cloud cover to facilitate clear satellite observations. Additionally, these dates followed consecutive days characterized by low average

wind speeds (< 3 m/s) to minimize resuspended silt and turbidity interference. Field measurements were taken in the morning during low-wave conditions (< 5 cm wave height) to ensure stable readings within the upper epilimnion.

Within the Holbina–SE_Razim study zone, measurements were made in 14 field station areas spanning a 12-km geographic gradient from the northwestern tip of Holbina Bay to the central part of Razim Lake. In each station area, drifting transects consisting of 3 to 13 sequential measurements were performed. The relative distance between successive measurements, sampled at 2-minute intervals, ranged from 30 to 100 m depending on the downwind boat drift velocity (which varied between 1 and 3 km/h). In total, a dataset of 97 discrete data points was established, capturing both [Chl-a] and [Phy] alongside supplementary water chemistry parameters.

Field measurements were collected at a water depth of 0.4–0.5 m using a SEBA KLL-Q-2 multiparameter system equipped with an MPS-K16 probe (SEBA Hydrometrie GmbH, Kaufbeuren, Germany). The probe configuration included dedicated sensors for in-vivo Chl-a and Phy fluorescence, alongside electrodes for water temperature, pH, electrical conductivity, oxidation-reduction potential, dissolved oxygen, nitrate, ammonium, and turbidity (Fig. 2). The SEBA fluorometer targets the in-vivo fluorescence of Chl-a (a photosynthetic pigment ubiquitous across phytoplankton taxa) and Phy (which, under Danube Delta conditions, serves as a distinct biomarker for cyanobacteria). Relative fluorescence units are automatically converted by the instrument software into pigment concentration equivalents (µg/L).

However, translating raw in-vivo fluorescence values into absolute concentrations introduces well-documented challenges compared to extraction-based methods (Brient et al. 2008; Rome et al. 2022). Although the SEBA firmware applies dynamic compensation algorithms utilizing the concurrent turbidity and temperature data streams, the resulting Chl-a and Phy estimations generally exhibit semi-quantitative to high accuracy profiles (R^2 = 0.70 to 0.96; Shivers et al. 2025). Consequently, a structurally significant component of the total variance observed in subsequent satellite-to-field correlations is expected to stem from this sensor-level uncertainty. Nevertheless, these high-resolution, in-situ fluorometric datasets provide robust internal consistency when utilized referentially to contrast localized lake zones, assess day-to-day dynamics, or trace macro-scale bloom gradients.

Following Randolph et al. (2008) and Haggard et al. (2023), algal blooms were classified as predominantly cyanobacterial when the [Phy]:[Chl-a] ratio exceeded 0.64. To characterize bloom intensity, we adopted established ecological awareness guidelines (Ahn et al. 2007; Brient et al. 2008; Staehr et al. 2010; Chorus & Welker 2021) using the following categorical thresholds:

- **Low baseline conditions:** < 10.0 µg/L Chl-a and/or < 2.0 µg/L Phy.
- **Mild cyanobacterial blooms:** 2.0-19.9 µg/L Phy.
- **Moderately severe blooms:** 10.0-50.0 µg/L Chl-a and/or 20.0-100.0 µg/L Phy.
- **High-risk SABs:** > 50.0 µg/L Chl-a and/or > 100.0 µg/L Phy.



Figure 2. The SEBA Hydrometrie KLL-Q2 measuring instrument.

Remote sensing estimation of surface water Chl-a and Phy was conducted using data from the Copernicus Sentinel-3 Ocean and Land Colour Instrument (OLCI), processed via custom-developed JavaScript workflows within the Google Earth Engine (GEE) platform. Top-of-atmosphere radiances were atmospherically corrected using a GEE-based Case 2 Regional CoastColour (C2RCC) emulator, followed by the application of the Normalized Difference Chlorophyll Index (NDCI) algorithm as a Chl-a proxy (Mishra & Mishra 2012). Conversely, atmospheric correction was bypassed for the Phycocyanin Index (PCI) calculation to preserve the weak phycocyanin signals following established protocols (Qi et al. 2014; Brockmann et al. 2016). To model the relationship between OLCI-derived NDCI and in-situ SEBA-[Chl-a] concentrations, our dataset was evaluated against the following empirical framework developed for optically complex, turbid productive waters (Mishra et al. 2014):

- **NDCI < 0.00:** < 14 ug/L Chl-a, (oligotrophic to mesotrophic conditions; low algal presence).
- **NDCI 0.00-0.10:** ~14.0–24.0 µg/L Chl-a (moderately productive waters).
- **NDCI 0.10-0.24:** ~24.0–46.0 µg/L Chl-a (high productivity; initial biomass buildup).
- **NDCI ≥ 0.25:** > 50.0 µg/L Chl-a (active bloom stage; severe algal bloom).

Although the original NDCI empirical framework proposed by Mishra et al. (2014) did not incorporate the C2RCC atmospheric correction algorithm (Müller et al., 2026), it remains widely adopted in contemporary literature for evaluating complex turbid waters (Watanabe et al., 2018; Al-Naimi et al., 2023).

For the relationship between OLCI-derived PCI and in-situ SEBA-[Phy] concentrations, our dataset was evaluated against the empirical framework established for highly eutrophic temperate lakes by Qi et al. (2014):

- **PCI > 0.95:** < 1.0 µg/L Phy (clear water conditions; minimal to no cyanobacteria present)
- **PCI 0.80-0.95:** 1.0–30.0 µg/L Phy (low to moderate blooms; eutrophic waters)
- **PCI 0.60-0.80:** 30.0–100.0 µg/L Phy (high biomass; initial cyanobacterial accumulation and potential bloom initiation)
- **PCI < 0.60:** > 100.0 µg/L Phy (severe cyanobacterial bloom)

To establish spatial correspondence between the in-situ SEBA measurements and satellite observations, field-determined GPS coordinates were paired with the overlapping Sentinel-3 pixel geometries. Historical NDCI and PCI reconstructions for the study area commenced on 25 August 2018, marking the initialization of the operational two-satellite Sentinel-3 constellation providing daily temporal resolution. The OLCI onboard Sentinel-3 features a nominal spatial resolution of 300 m. To eliminate confounding spectral contamination from shoreline and emergent macrophyte vegetation, the lake margin boundaries were manually digitized and masked out of the final analysis.

RESULTS AND DISCUSSIONS

The elevated phycocyanin concentrations captured across all sampling stations between 11 and 13 August 2026 (overall mean: 153.7 ± 80.8 µg/L; range: 12.9-366.7 µg/L), coupled with high [Phy]:[Chl-a] ratios spanning 2.18 to 23.04, confirm the occurrence of a widespread cyanobacterial SAB throughout the Holbina–SE_Razim aquatic system. Conversely, the observed NDCI values remained low, which mathematically corresponds to low-to-moderate chlorophyll-a levels under standard empirical baselines (Mishra & Mishra, 2012).

A distinct spatial divergence in bloom intensity and pigment distribution was observed between the two water bodies:

- **Holbina Bay:** Characterized by lower baseline concentrations, exhibiting a mean Chl-a of 8.78 ± 1.98 µg/L and a mean Phy of 14.78 ± 4.40 µg/L.
- **SE Razim Lake:** Exhibited high-risk, intense bloom conditions, with a mean Chl-a of 84.90 ± 30.72 µg/L and a massive mean Phy of 242.72 ± 65.04 µg/L.

Welch's t-test confirmed that the mean concentrations of both pigments were significantly different between Holbina Bay and SE Razim Lake ($p < 0.001$). A strong, positive linear correlation was observed between overall [Chl-a] and [Phy] ($r = 0.899$; $p < 0.0001$; $N = 97$), with $r = 0.76$, $p < 0.0001$ and $N = 47$ in Holbina, and $r = 0.942$, $p < 0.0001$ and $N = 50$ for SE_Razim (Fig. 3). When analyzed by region, this robust coupling was maintained in both Holbina Bay ($r = 0.76$, $p < 0.0001$, $N = 47$) and SE_Razim Lake ($r = 0.942$, $p < 0.0001$, $N = 50$; Fig. 3). However, this tight correlation may be rooted in an optical artifact at 665 nm induced by the exceptionally high [Phy]:[Chl-a] ratio.

A graphical observation of [Chl-a] against [Phy] demonstrated that despite their wide hydrographic continuity, these two water bodies exhibited distinct [Chl-a] to [Phy] structural relationships. To evaluate this divergence, a test for the homogeneity of regression slopes was performed (Zar 2010), a technique routinely applied in comparative algal bloom dynamics (Oleksy et al. 2021). The analysis revealed that the two regression slopes were significantly different ($p = 0.0255$, $n_1 = 47$, $n_2 = 50$). This structural divergence confirms that the analyzed SAB encompassed a distinct spatial gradient in taxonomic composition or bloom maturity phase.

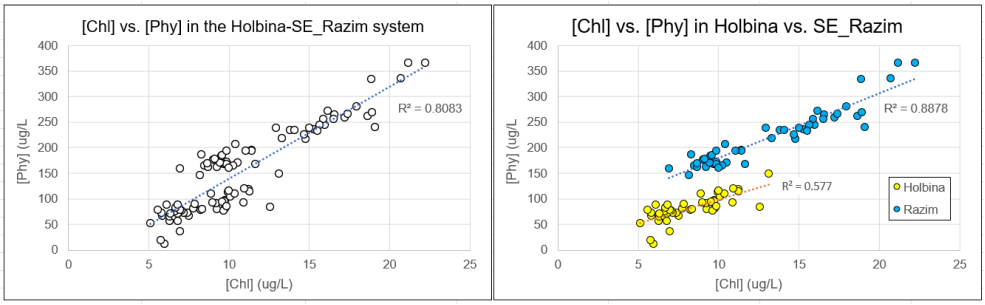


Figure 3. Bivariate linear regression analysis of in-situ pigment relationships during the 11–13 August 2026 severe algal bloom (SAB) within the Holbina-SE_Razim system. (Left) Overall linear relationship between chlorophyll-a ([Chl-a]) and phycocyanin ([Phy]) concentrations across the entire dataset (N = 97). (Right) Distinct, localized regression lines computed separately for Holbina Bay (n_1 = 47) and SE Razim Lake (n_2 = 50), demonstrating the statistically significant spatial divergence in the [Chl-a] to [Phy] slope.

When comparing the field-based fluorescent measurements of algal pigments ([Chl] and [Phy]) with the corresponding Sentinel-3 parameters NDCI and PCI, we found no correlation over the full [Chl]-measured domain (5.1 to 22.2 µg/L) and NDCI (r = 0.03; p = 0.77; N = 97), and strong negative linear correlation between the full [Phy]-measured domain (12.97 to 366.7 µg/L) and PCI (r = 0.553; p < 0.0001; N = 98), (Fig. 4).

When validating the in-situ fluorometric pigment concentrations against their corresponding Sentinel-3 OLCI parameters, the full-domain analysis yielded highly contrasting results for the two indices. No statistically significant correlation was observed between the complete Chl-a range (5.1-130.0 µg/L) and the NDCI (r = 0.03, p = 0.77, N = 97). Conversely, a robust and statistically significant negative linear correlation was established between the full Phy concentration domain (12.9-366.7 µg/L) and the PCI (r = -0.553, p < 0.0001, N = 97; Fig. 4). However, the empirical PCI-to-[Phy] coordination thresholds observed in the Holbina-SE_Razim system diverged significantly from the baseline criteria established by Qi et al. (2014). Instead, our dataset yielded the following localized linear predictive model:

[Phy] (µg/L) = -1658.6 PCI + 1384.5.

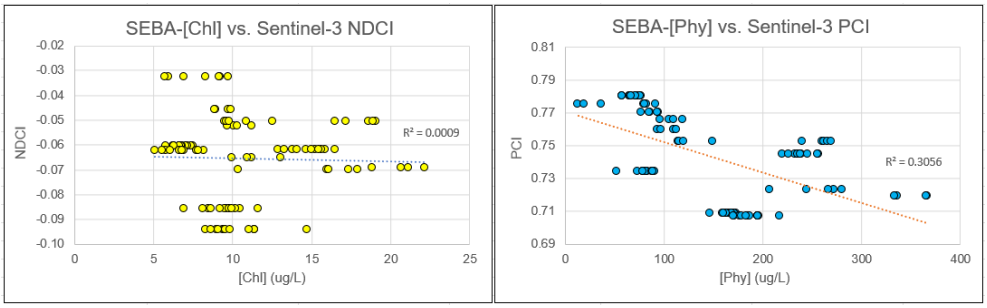


Figure 4. (Left) Relationship between in-situ SEBA-[Chl-a] concentrations and Sentinel-3 NDCI values during the 11–13 August 2026 severe algal bloom (SAB). (Right) Relationship between in-situ SEBA-[Phy] concentrations and Sentinel-3 PCI values during the same campaign.

This discrepancy underscores the need for regional calibrations to accurately characterize the [Phy]/PCI relationship under the specific conditions of Danube Delta lakes.

To identify the maximum Chl-a range yielding a statistically significant [Chl-a]/NDCI relationship, we performed a Moving Window Linear Regression Optimization (MW-LRO). This algorithmic optimization approach was previously used for validating satellite products against algal blooms (Groetsch et al. 2016). Imposing a strict significance threshold of $p < 0.01$, the MW-LRO revealed no optimal range within the -0.0691 to -0.0326 NDCI domain, corresponding to the 5.1–21.15 µg/L [Chl-a] interval. While the standard baseline from Mishra & Mishra (2012) dictates that a positive correlation should emerge at concentrations exceeding 22.0 µg/L, the [Chl-a] values in this SAB remained exceptionally low. Conversely, applying the MW-LRO to the PCI versus [Phy] dataset yielded no statistical improvement over any localized subdomain, confirming that the negative linear correlation remains uniformly valid across the entire 13.0–366.0 µg/L [Phy] range.

To resolve the discrepancy between literature-supported baseline trends and our empirical findings, multivariate analyses were performed to isolate patterns across specific locations and sampling dates. Figure 5 (Left) illustrates the dissimilarities among the four primary sub-samples. The dataset was subsequently reorganized to evaluate changes in the [Chl-a]/NDCI correlation when grouping the transitional station Holbina_St5_20260813 with the SE_Razim cluster, or when isolating distinct local outliers. Guided by the 8-year historical PCI map pixel averages (25 August 2018 to 25 August 2026), we also re-grouped stations Holbina_St10_20260813 and Holbina_St4_20260813 with the SE_Razim domain. This eco-geographic stratification revealed a statistically significant positive correlation between [Chl-a] and NDCI (Fig. 5, Right). Specifically, the correlation was robust for both the northwestern-to-mid Holbina Bay cluster ($r = 0.49$, $p = 0.0016$, $N = 34$) and the SE_Razim group ($r = 0.46$, $p < 0.0001$, $N = 64$). Sizable scattering was restricted to the anomalous station Holbina_St1. Given its unique localized attributes (characterized by exceptionally low pigment concentrations, shallow depths, high Secchi disk transparency, and dense submerged macrophytes) this atypical micro-habitat should be omitted from future macro-scale satellite validation campaigns within the broader Holbina–SE_Razim system.

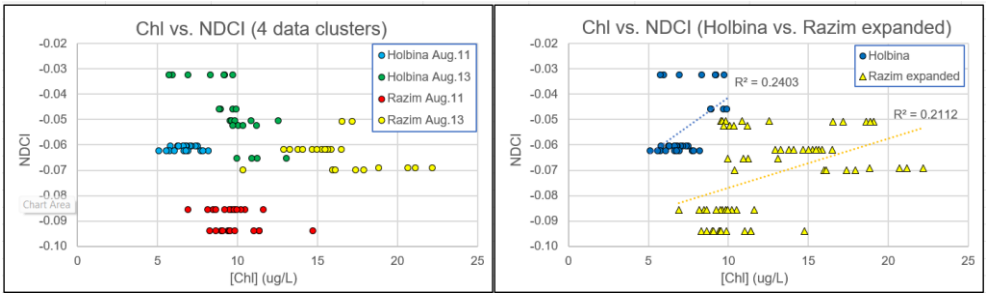


Figure 5. Bivariate distribution of [Chl-a] versus NDCI during a severe algal bloom (SAB) event. (Left) Initial dataset clustered by lake domain and sampling date, demonstrating significant spatio-temporal dissimilarities among the four sub-samples. (Right) Optimized linear relationships following eco-geographical data stratification into two distinct groupings: Group 1 (Holbina Bay; comprising northwestern and central stations) and Group 2 (Razim; comprising the southeastern Razim basin and transitional southeastern Holbina Bay stations).

Based on these patterns, we hypothesized that the degradation of the overall [Chl-a]/NDCI correlation across the entire Holbina–SE_Razim dataset resulted from mixing data from two distinct SAB types or phases, compounded by an asymmetric sampling effort. To test this hypothesis, we ranked the sampling stations along a continuous geographic transect starting from the north-northwest to the east-southeast of Holbina Bay, and extending westward into central Razim Lake. We then applied a stepwise data-removal protocol, tracking the [Chl-a] versus NDCI correlation within the remaining data subsets. Prior to the exclusion of station Holbina_St2_20260811, the variables exhibited no statistically significant relationship ($p > 0.05$). At this exclusion threshold, however, the [Chl-a]/NDCI correlation became robust and positive ($p < 0.0001$, $N < 60$). The strongest correlation was seen in the SE_Razim Lake once all Holbina Bay data points were removed ($r = 0.766$, $p < 0.0001$, $N = 50$).

Two additional bio-optical mechanisms likely contributed to the degradation of the [Chl-a]/NDCI correlation across the Holbina-SE_Razim system. These factors directly influence the water-leaving radiances within the Sentinel-3 OLCI spectral bands utilized in the NDCI framework:

$$NDCI = (R_{rs}(708)-R_{rs}(665)) / (R_{rs}(708)+R_{rs}(665)))$$

In typical chlorophyll-dominated waters, rising [Chl-a] drives an increase in pigment absorption at 665 nm (reducing reflectance), while simultaneous cellular backscattering elevates reflectance at 708 nm. This contrasting spectral behavior forces the NDCI value upward into a positive range that correlates linearly with [Chl-a]. In theory, Razim Lake SABs could exhibited two features capable of disrupting this relationship:

(1) Phycocyanin absorption overlap: An exceptionally high [Phy] can expand the absorption wing of the 620 nm Phy into the 665 nm channel. This spectral overlap can introduce noise into the Chl-a signal, artificially pushing the NDCI toward negative values.

(2) Suspended sediment interference: The expansive yet shallow Razim Lake is highly susceptible to wind-driven sediment resuspension. When this happens, elevated inorganic turbidity can shift the background reflectance baseline, forcing the NDCI toward negative values, even as algal biomass accumulates.

While the contribution of these bio-optical factors cannot be entirely dismissed, the most pronounced disruption of the [Chl-a]/NDCI correlation occurred within Holbina Bay, the specific zone where phycocyanin concentrations were consistently and significantly lower than in the SE Razim basin. Furthermore, any confounding turbidity bias was likely minimal during our campaign, as evidenced by a significant spatial decrease in turbidity toward the sheltered interior of Holbina Bay (data not shown). Consequently, our findings show that pooling field data across bloom areas that are distinct in taxonomic structure or bloom maturity phases, or employing asymmetrical sampling designs, can introduce greater noise into the [Chl-a]/NDCI correlation than the presence of an extreme [Phy]/[Chl-a] ratio alone, even at [Phy]:[Chl-a] ratios spanning 2.2 to 14.6.

Lastly, similarities between the field sampling stations were evaluated to develop a robust sampling optimization strategy. We employed a multivariate normalized analysis approach, followed by Neyman optimal allocation of sampling efforts, a framework previously implemented in satellite post-processing for algal bloom monitoring (Flener & Calomeni 2025; Ramirez-Perez et al. 2025). Ten stations

sampled on a single day (13 August) were compared across five distinct variables: [Chl-a], [Phy], [Phy]/[Chl-a], NDCI/[Chl-a], and PCI/[Phy]. The results demonstrated that [Phy] concentration was the most robust station discriminator (F = 212.72), with inter-station variability vastly exceeding the internal variance introduced by replicate sampling within each station. This was followed by the [Phy]/[Chl-a] parameter (F = 63.28) and the NDCI/[Chl-a] parameter (F = 11.89), with noise levels increasing progressively across each station. Based on a comparison of mean Z-scores, the station Holbina_St1 was isolated as a uniquely highly variable habitat. It was followed sequentially by the remaining low-productivity Holbina Bay stations (No.: 2, 3, 4, 5, and 10), and lastly by the stable SE Razim Lake stations (No.: 6, 7, 8, and 9). Multi-dimensional scaling and station cluster analysis revealed no crossover between groups, confirming zero spatial misclassification between the Holbina and Razim data subsets.

Our results demonstrate that the two studied water bodies, Holbina Bay and SE_Razim Lake, exhibit ecologically distinct SABs, characterized by highly divergent Phy features. Spatially, the field stations bridging the statistical and ecological gap between the two basins were Holbina_St5 and Razim_St9. To optimize future monitoring, an optimal stratified sampling design was computed using Neyman's allocation formula. For a hypothetical verification campaign with a planned baseline of 60 field measurements, the model allocated sampling efforts as follows: 24 discrete measurements concentrated within the highly variable, localized Holbina_St1 habitat, and 4 measurements distributed uniformly across each of the 9 remaining stations. Based on these optimization metrics, we propose the following multi-tiered strategy for investigating future SAB dynamics across the 100-km² Holbina–SE_Razim aquatic system:

1. **Identify SAB events:** Screen incoming Sentinel-3 OLCI imagery to detect initial SAB formations.
2. **Generate baseline index maps:** Process the raw imagery into localized NDCI and PCI pixel distribution maps.
3. **Construct contour intervals:** Generate NDCI and PCI contour maps utilizing fixed 5% percentage intervals to visualize spatial gradients.
4. **Target dynamic field zones:** Delineate field target zones based on spatial variations (dNDCI and dPCI) and calculate the relative abundance of the 5% dissimilar surface areas.
5. **Define sampling thresholds:** Establish the total field sampling volume (number of stations and localized replicates) based on prior empirical variance and logistical resources.
6. **Deploy spatial grids:** Generate and distribute precise GPS station coordinates across the targeted zones to guide the field crew or automated platforms.
7. **Execute field measurements:** Collect in-situ pigment data within the established coordinates utilizing either traditional vessel-based sampling or pre-programmed surface drones.
8. **Perform same-day recalibrations:** Calibrate concurrent same-day Sentinel-3 reads against the fresh field measurements to update regression coefficients for the specific bloom type, phase and local conditions.
9. **Map absolute concentrations:** Apply the freshly updated empirical models to the daily Sentinel-3 data streams to produce high-resolution, absolute concentration maps of [Chl-a] and [Phy].

10. **Iterate until bloom clearance:** Repeat the entire spaceborne-to-field sequence dynamically on daily operational loops until total SAB extinction.

This hybrid operational strategy successfully leverages the complementary strengths of satellite remote sensing and high-resolution in-situ measurements, optimizing the capacity to track, model, and predict the complex evolution of SABs in highly dynamic aquatic ecosystems.

CONCLUSIONS

Using the Holbina-SE_Razim lake system as a natural laboratory, we validated satellite-derived algal pigment observations against a robust spatial gradient of field-based Chl-a and Phy measurements. This study demonstrates that in freshwater deltaic ecosystems (such as Danube Delta lakes), variations in bloom-related pigment features introduce significant biases into the NDCI/Chl-a relationship. Despite a broad physical connection, multi-temporal satellite analyses revealed highly distinct, contrasting algal bloom dynamics between Holbina Bay and southeastern Razim Lake. Stratifying the data across these ecological boundaries confirmed that consistent variations in pigment concentrations and ratios match historical pigment patterns. Crucially, our results underscore that rigorous historical data screening and in-field measurements are prerequisites for isolating and interpreting distinct bloom patterns. The validated Sentinel-3 framework, specifically the Sentinel-3 PCI parameter, offers a scalable tool for monitoring water quality and capturing the evolution of severe cyanobacterial blooms in large freshwater systems.

ACKNOWLEDGMENT

Sentinel-3 OLCI data were provided by the European Union/ESA/Copernicus program and accessed/processed through the Google Earth Engine platform. The authors gratefully acknowledge the open data policy of Copernicus and the cloud-computing support provided by Google Earth Engine. This work was supported by a grant of the Ministry of Research, Innovation and Digitalization from Romania, UEFISCDI, project number PN-IV-PCB-RO-MD-2024-0152, within PNCDI IV, and by the National Agency for Research and Development (ANCD) of the Republic of Moldova, project number 25.80013.5107.28ROMD, under the bilateral cooperation framework.

REFERENCES

Ahn C.-Y., Joung S.-H., Jeon J.-W., Jang M.-H., Oh H.-M., 2007, Alternative alert system for cyanobacterial bloom, using phycocyanin as a level determinant, The Journal of Microbiology, 45(2):98-104.

Al-Naimi, H. A., et al., 2023, Validation of Sentinel-3 OLCI water color products over highly turbid estuarine waters using the C2RCC processor. Environmental Monitoring and Assessment, 195(4), 482.

Brient L., Lengronne M., Bertrand E., Rolland D., Sipel A., Steinmann D., Baudin I., Legeas M., Le Rouzic B., Bormans M., 2008, A phycocyanin probe as a tool for monitoring cyanobacteria in freshwater bodies, Journal of Environmental Monitoring, 10(2):248-255.

Chorus I., Welker M., 2021, Toxic Cyanobacteria in Water: A guide to their public health consequences, monitoring and management, World Health Organization (WHO).

Flener, A., & Calomeni, A. J., 2025, Machine learning and adaptive monitoring for harmful algal blooms under optimized sample budgets. Estuaries and Coasts, 48(2), 162–177.

Groetsch P. M., Simis S. G., Bryan A. M., Robertson J. E., Peters S. W., 2016, Spring blooms in the Baltic Sea have weakened but lengthened from 2000 to 2014, Biogeosciences, 13(17):4959-4973.

Haggard B. E., Grantz E., Austin B. J., Wagner N. D., Scott J. T., 2023, Chlorophyll and Phycocyanin Raw Fluorescence May Inform Recreational Lake Managers on Cyanobacterial HABs and Toxins: Lake Fayetteville Case Study, Journal of Contemporary Water Research & Education, 177:63-71.

Matthews M. W., Bernard S., Winter A., 2012, A remote sensing phenology of cyanobacteria blooms in a hypertrophic lake using MERIS, Remote Sensing of Environment, 124:637-652.

Mishra S., Mishra D. R., 2012, Normalized difference chlorophyll index: A novel model for remote estimation of chlorophyll-a concentration in turbid productive waters, Remote Sensing of Environment, 117:394-406.

Mishra D. R., Schaeffer B. A., Keith D., 2014, Performance evaluation of normalized difference chlorophyll index in northern Gulf of Mexico estuaries using the Hyperspectral Imager for the Coastal Ocean, GIScience & Remote Sensing, 51(2):175-198.

Müller, D., Hieronymi, M., Ruescas, A. B., Peters, M., Röttgers, R., König, M., Lebreton, C., Stelzer, K., Brockmann, C., & Doerffer, R., 2026, Case 2 Regional Coast Colour: a neural network-based framework for atmospheric correction and in-water retrievals across multiple ocean colour satellite sensors. Frontiers in Remote Sensing, 7: Article 1710758.

Oleksy I. A., Baron J. S., Spaulding S. A., 2021, Nutrients and warming alter mountain lake benthic algal structure and function, Freshwater Science, 40(1):88-102.

Qi L., Hu C., Duan H., Cannizzaro J., Ma R., 2014, A novel MERIS algorithm to derive cyanobacterial phycocyanin pigment concentrations in a eutrophic lake: Theoretical basis and practical considerations, Remote Sensing of Environment, 154:298-317.

Pérez-Vega, A., Mas, J.-F., Delegido, J., & Ruiz-Verdú, A., 2026, Optimizing sampling design for chlorophyll-a estimation in inland waters using Sentinel-2 imagery and spatial clustering. International Archives of the Photogrammetry, Remote Sensing and Spatial Information Sciences, XLVIII-3/W4-2025, 33–40.

Randolph K., et al., 2008, Hyperspectral remote sensing of cyanobacteria in turbid productive water using optically active pigments, chlorophyll a and phycocyanin, Remote Sensing of Environment, 112(11):4009-4019.

Rome M., Beighley R. E., Faber T., 2021, Sensor-based detection of algal blooms for public health advisories and long-term monitoring, Science of The Total Environment, 767:144984.

Staehr P. A., et al., 2010, Ecosystem metabolism in shallow lakes: the importance of sampling frequency and use of a metabolic model, Limnology and Oceanography: Methods.

Zar J. H., 2010, Biostatistical Analysis (5th ed.), Prentice Hall. (Specifically Chapter 18: "Comparing Two Linear Regression Equations").

Watanabe, F. S., Alcantara, E., Rodrigues, T. W., Rotta, L. H., Bernardo, N., & Carmo, M. S., 2018, Estimation of chlorophyll-a concentration in a eutrophic reservoir using C2RCC-processed Sentinel-2 MSI images. Remote Sensing Applications: Society and Environment, 12, 103-113.